

**Observation of depinning phenomena in the sliding friction of Kr films on gold**

A. Carlin, L. Bruschi, M. Ferrari, and G. Mistura

*Istituto Nazionale per la Fisica della Materia and Dipartimento di Fisica G. Galilei, Università di Padova, via Marzolo 8, 35131 Padova, Italy*

(Received 28 February 2003; published 25 July 2003)

We have used quartz crystal microbalance to study the sliding friction of atomically thin Kr films adsorbed on gold. We have observed sharp pinning transitions separating a low-coverage region, characterized by slippage at the solid-fluid boundary, from a high-coverage region where the film is locked to the oscillating electrodes. Furthermore, we have induced sliding of a film by slowly increasing the amplitude of the substrate oscillations. Such a depinning transition is characterized by hysteresis as the amplitude is decreased back to zero. These observations have been obtained with two different quartz plates and are similar to those recently reported in the literature. A more quantitative comparison among the different experimental runs indicate that the location of these dynamical transitions is strongly dependent on the state of the substrate surface.

DOI: 10.1103/PhysRevB.68.045420

PACS number(s): 68.35.Af, 68.35.Rh, 81.40.Pq

**I. INTRODUCTION**

The dynamic response of various condensed-matter systems interacting with pinning potentials exhibits a very rich, nonlinear behavior.<sup>1</sup> A small applied force  $F$  is not sufficient to overcome the random pinning centers and the system remains trapped. By increasing  $F$ , a threshold value  $F_c$  is reached above which the system is moving. Such a depinning transition can be either continuous or first order with hysteresis.<sup>2</sup> Examples of such systems include vortex lattices in type-II superconductors,<sup>3</sup> charge-density waves in anisotropic conductors,<sup>4</sup> motion of contact lines of droplets on rough substrates<sup>5</sup> and of an interface in a random medium,<sup>6</sup> and two-dimensional (2D) colloidal systems on disordered substrates.<sup>7</sup>

Arguably, the paradigm of a system undergoing depinning is an adsorbed monolayer sliding onto a substrate.<sup>8</sup> The model system of an overlayer of interacting particles attracted by a substrate potential and subject to an external driving force has been extensively studied through molecular dynamics.<sup>9–12</sup>

In particular, simulations based on Brownian-motion dynamics and carried out by Persson<sup>9</sup> show a rich phenomenology. On a weakly corrugated, periodic substrate, a film is always found to slide no matter how small the applied force is. Instead, on strongly corrugated film-substrate potentials, the film slides whenever it is in a fluid phase. However, if the film is solidlike, the nanofriction exhibits a sharp depinning transition characterized by hysteresis as the pulling force is decreased back to zero. The use of a disordered substrate does not seem to preclude the observation of such a nonlinear behavior, as long as a solid adsorbate structure occurs for  $F = 0$ .

Recent experiments seem to confirm this picture. The shear response of molecularly thin liquid films on solid substrates when subjected to an applied air stress has been measured and found to correspond to viscous friction.<sup>13</sup> Vice versa, investigations with a quartz-crystal microbalance of Kr films adsorbed on gold at low temperatures and likely to be solidlike may display static friction under certain conditions.<sup>14</sup> In the following, we will show further data ac-

quired with two different quartz crystals that present similar depinning transitions in the nanofriction of Kr films on gold.

This paper is organized as follows. After a detailed discussion of the experimental setup and data acquisition procedures followed in our measurements, we present a simple normalization of the derived slip times, which we feel is more realistic to quantify the dynamic response of a submonolayer film. We then describe the friction data acquired with two different quartz crystals, comparing in some detail the depinning phenomena observed with each sensor. Finally, we put in evidence how the state of the adsorption surface plays a crucial role in this kind of phenomena.

**II. EXPERIMENTAL SETUP AND DATA ACQUISITION**

The microbalance is a small AT-cut quartz disk whose principal faces are optically polished and covered by two gold films, which are used both as electrodes and as adsorption surfaces. By applying an ac voltage across the two electrodes, it is possible to drive the crystal to its own mechanical resonance with the two parallel faces oscillating in a transverse shear motion, characteristic of the AT cut. The quality factor of these resonances is usually very high ( $\geq 10^5$ ) and this explains why the quartz-crystal microbalance (QCM) is a quite sensitive probe of interfacial phenomena. In particular, it has been successfully applied to the study of nanofriction of physisorbed films,<sup>15</sup> because it detects both coverage and interfacial viscosity. A change in the disk inertia, as caused, for example, by the adsorption of a film on the metal electrodes, is signaled by a shift in the resonant frequency. Similarly, any dissipation taking place in the system causes a decrease in the resonance amplitude.

The acoustics of the quartz-film-vapor system can be solved using the Navier-Stokes equations simplified for incompressible fluids,<sup>16</sup> leading to the determination of the slip time  $\tau$  which describes the viscous coupling between the gold substrate and the physisorbed film. The meaning of this quantity is quite intuitive, since it represents the time constant of the exponential film velocity decrease due to an hypothetical sudden stop of the oscillating substrate. Very low slip times mean high interfacial viscosity and, in the extreme

case of a film rigidly locked to the substrate,  $\tau$  goes to zero. In the opposite case of a superfluid, whose motion is totally decoupled from that of the underlying substrate,  $\tau \rightarrow \infty$ . Typical values of  $\tau$  in the case of a rare-gas film adsorbed on gold are generally comprised between 1 and 10 ns.

Here we present data acquired using two different quartz plates: quartz 1, which has been employed in a previous study,<sup>14</sup> has a resonance frequency of 6 MHz, while quartz 2 has a frequency of 5 MHz; both of them are characterized by quality factors  $\geq 10^5$  in vacuum and at low temperature. The data we present refer only to the fundamental mode. The resonance frequency and amplitude are measured by means of a frequency modulation technique, in which the output signal of a radiofrequency (r.f.) generator is locked onto the peak resonance.<sup>17</sup> The sample is mounted in a brass cell, installed in a homemade liquid-nitrogen cryostat and directly connected to a turbomolecular pump through a short stainless-steel tube in order to reach a high pumping speed.

In this study we have performed two kinds of measurements: isothermal coverage scans and isothermal amplitude scans. In both cases we detect the frequency and the amplitude shifts of the resonance peak from their vacuum values. In the first case the gas is admitted into the sample cell in small doses up to its saturated vapor pressure  $P_{\text{sat}}$ . Every time the pressure is increased, the system reaches equilibrium after a short transient and the corresponding quartz resonance parameters are recorded. Figure 1 shows an isotherm of Kr on gold taken at  $T=85$  K following such a procedure. In particular, the two top graphs display the measured frequency  $f_{\text{meas}}$  and voltage  $V_{\text{meas}}$  values of the quartz crystal as a function of the vapor pressure. The horizontal log scale is used only for clarity reasons. From the corrected shifts of frequency and voltage with respect to the corresponding values in vacuum, it is then possible to determine the slip time and the film coverage according to the formulas described in Ref. 16. The result of such analysis is shown in the bottom graph of Fig. 1. We point out that the jump in slip time is related to the step observed in the amplitude graph (see Sec. IV for further details).

The second possible way to acquire data consists in an amplitude scan: the crystal is driven to resonance using different voltages which are changed by varying the output signal of the r.f. generator. Since the oscillating amplitude  $A$  of the metal electrodes depends on the driving voltage, it is then possible to vary in a precise way the amplitude of the force of inertia  $F=4\pi^2 m A f^2$  acting on each adsorbate molecule of mass  $m$  tangentially to the gold surface. The data acquisition is fully automatized and controlled via computer. The actual value of the electrode displacement  $A$  is deduced from the voltage applied across the electrodes  $V_{\text{quartz}}$  once the resonance quality factor has been measured.<sup>18</sup> In our case,  $V_{\text{quartz}}$  is comprised between 1 and 6 mV and the induced displacements are in the range 1.5–10 Å. For this procedure, a scan in vacuum is first taken as a reference: the resonance parameters are measured as a function of the output power of the r.f. generator. The data acquisition is then repeated after the admission in the sample cell of a known amount of gas and is carried out both at increasing and at decreasing power.

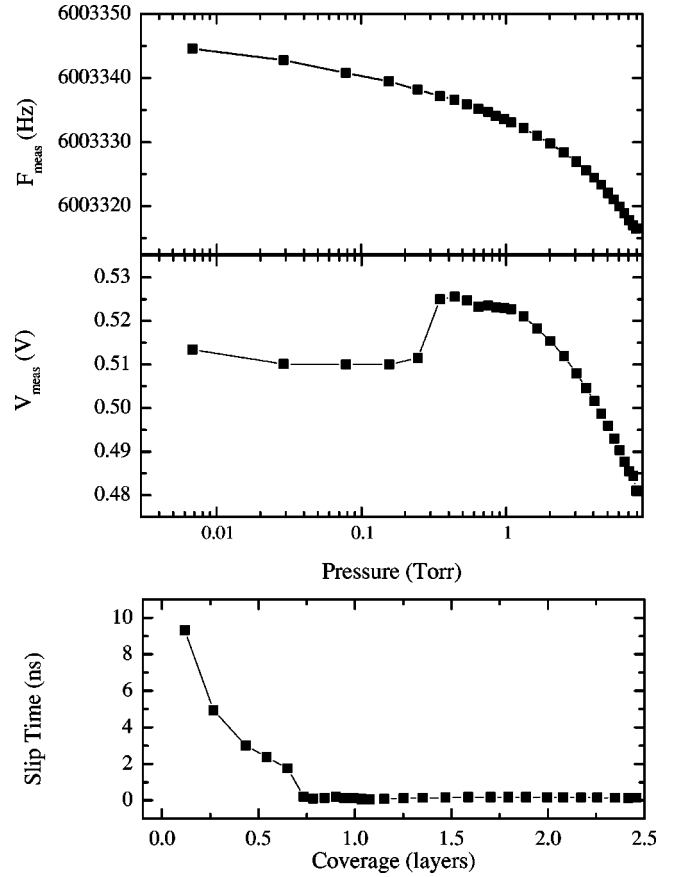


FIG. 1. Raw data of the resonance frequency (top) and amplitude (middle) measured with quartz 1 during an adsorption isotherm of Kr on gold at 85 K. Bottom: calculated slip time as a function of Kr film coverage.

Figure 2 shows an example of such a procedure. The top graph indicates the dependence of  $V_{\text{quartz}}$  as a function of the increasing output voltage of the r.f. generator, in vacuum and with a Kr film of 0.7 layers covering the gold electrodes. The inset shows an enlargement of the interesting part of the curves, where the gap between the two suddenly increases. The corresponding frequency datasets are instead separated by an almost constant amount which is barely visible over the amplitude range of Fig. 2 and for this reason have not been plotted. For each driving voltage, a slip time has been calculated from the frequency and voltage shifts with respect to the corresponding vacuum values using the same formulas mentioned before. The result of this analysis is the bottom graph, where the calculated slip time is plotted as a function of the oscillating amplitude of the gold electrodes.

### III. NORMALIZATION OF THE SLIP TIME

All of the theoretical analyses of the interfacial slippage between a thin film and an oscillating metallic substrate rely on the slab model:<sup>16,19</sup> a film covers uniformly the electrode surface area  $S_{\text{elec}}$ , its equivalent thickness being calculated from the formula  $m_{\text{film}} = \rho_{\text{film}} S_{\text{elec}} d$ . The quantity  $\rho_{\text{film}}$  is the mass density of the film, usually assumed equal to that of the bulk liquid (solid) at the same temperature. The friction force at the solid-film interface is given by

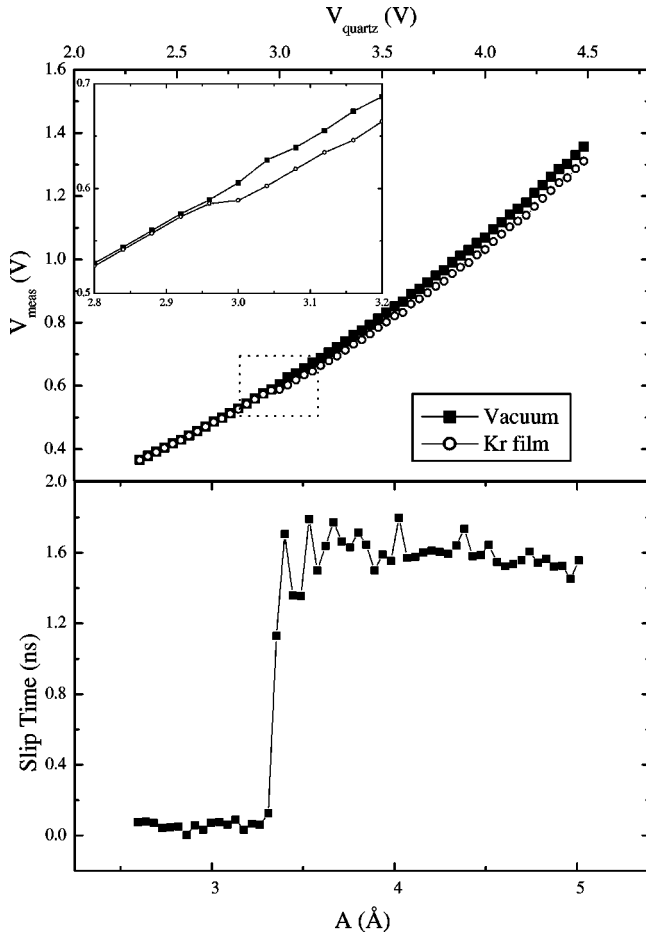


FIG. 2. Top: raw data of the resonance amplitude, measured with quartz 1 in vacuum and in the presence of 0.7 layers of Kr, as a function of the increasing generator output. Bottom: calculated slip time as a function of the oscillating amplitude of the quartz electrodes.

$$F_{\text{fric}} = -\eta_{\text{slab}} S_{\text{elec}} (v_{\text{film}} - v_{\text{elec}}) \quad (1)$$

which implicitly defines the interfacial viscosity  $\eta_{\text{slab}}$ . From the acoustical analysis of the combined quartz-film-vapor system model, such a quantity is also related to the decrease in amplitude of the oscillator via the acoustic resistance of the system. Accordingly, the slip time can be derived by the relation

$$\tau_{\text{slab}} = \rho_{\text{film}} d / \eta_{\text{slab}}. \quad (2)$$

In reality, if the film coverage is less than 1 monolayer, there will be regions of the electrodes surface covered with atoms and others free. In other words, the true contact area will be less than that geometric. In order to be consistent with this picture, formula (1) has to be rewritten as

$$F_{\text{fric}} = -\eta S_{\text{contact}} (v_{\text{film}} - v_{\text{elec}}) \quad (3)$$

and thus the corresponding slip time becomes

$$\tau = \rho_{\text{film}} d / \eta. \quad (4)$$

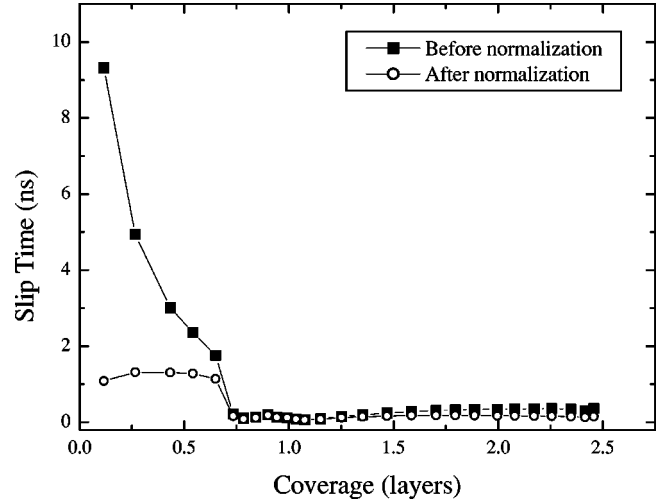


FIG. 3. Slip time of Kr on gold measured at 85 K with quartz 1, before and after the normalization procedure.

Obviously, the total friction force at the interface must be the same in the two cases, since what we measure is the value of  $F_{\text{fric}}$ , and then

$$\tau = \tau_{\text{slab}} \eta_{\text{slab}} / \eta = \tau_{\text{slab}} S_{\text{contact}} / S_{\text{elec}} = \tau_{\text{slab}} \Delta f / \Delta f_1, \quad (5)$$

where  $\Delta f$  represents the measured frequency decrease corrected for the hydrostatic effect and the viscous coupling to the vapor<sup>16,19</sup> and  $\Delta f_1$  is the frequency shift expected for the adsorption of the first monolayer.

The above equation is valid for coverages less than 1 monolayer. Instead, for thicker solid films, the slip time is normalized according to the formula<sup>21</sup>

$$\tau = \tau_{\text{slab}} \Delta f_1 / \Delta f \quad (6)$$

which explicitly takes into account the fact that the friction force is generated at the interface between the substrate and the adsorbate.

In the following graphs, we show the results of this normalization to some real datasets. Figure 3 refers to the same experimental run illustrated in Fig. 1, before and after normalization. The two curves coincide at high film coverages, while they are significantly different at lower values.

Similarly, Fig. 4 shows a set of amplitude scans taken at three different coverages before (top graph) and after (bottom graph) the same normalization procedure. The dataset corresponding to 0.7 layers is the same of Fig. 2. Above the jumps, the normalized slip times are close to each other, instead  $\tau_{\text{slab}}$  differs by more than a factor of 3 between 0.2 and 0.7 layers.

#### IV. EXPERIMENTAL RESULTS

The isotherms presented in the previous graphs display a jump separating a low coverage region, characterized by slippage at the solid-fluid boundary, from a high coverage region where the film, within our resolution, is locked to the oscillating electrodes. This behavior is similar to what we recently observed in our laboratory.<sup>14</sup> An analogous pinning

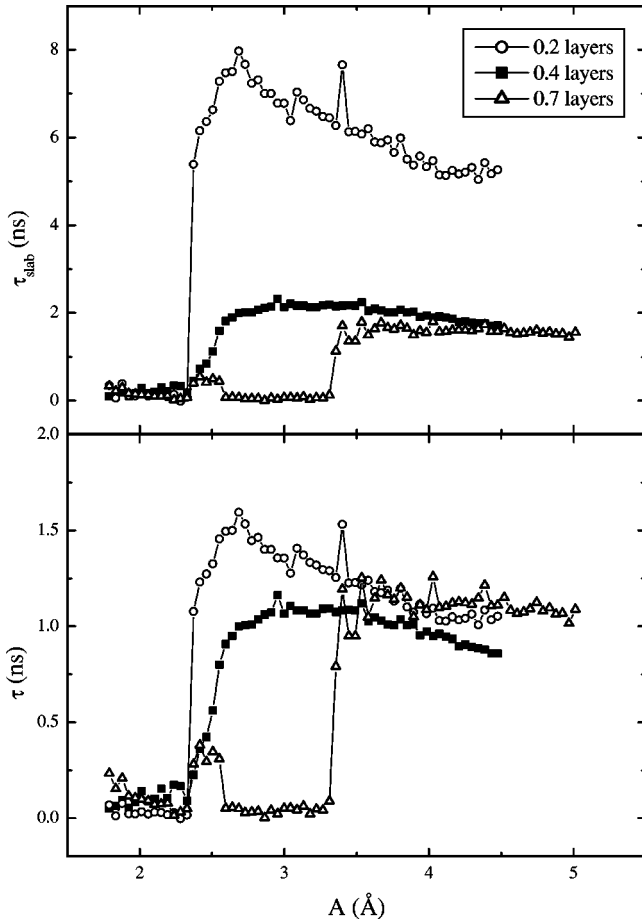


FIG. 4. Amplitude scans of Kr on gold measured with quartz 1 at 85 K for three Kr coverages before (top) and after (bottom) the normalization procedure. For clarity reasons, only the data at increasing amplitude are shown.

transition may have also been seen by Krim and co-workers in a QCM study of Kr on silver, although the authors did not make any specific comment about the presence of a sudden jump in one of the published isotherms.<sup>20</sup> The fact that, except this possible case of pinning, they always find sliding of Kr on gold is probably due to the larger driving amplitudes used in these measurements.<sup>19,20</sup>

Actually, the position of the pinning transition observed during a coverage scan is found to depend on the oscillating amplitude of the electrodes. Figure 5 shows a set of Kr isotherms measured with quartz crystal 2 at 97 K and corresponding to three different amplitudes. The slip time is normalized as explained in the previous section and the coverage is plotted in a log scale for clarity reasons. At low coverage, the curves practically coincide; as the coverage increases, they show a broad maximum just before the pinning transition. Interestingly, we notice that such a transition is steplike at low amplitude and becomes distinctly more rounded at higher  $A$ . Similar behavior has been observed with other quartz crystals. Currently, we are taking more systematic data in order to better characterize this change in slope.

As mentioned earlier, a different way to take data consists in amplitude scans at constant temperature and film cover-

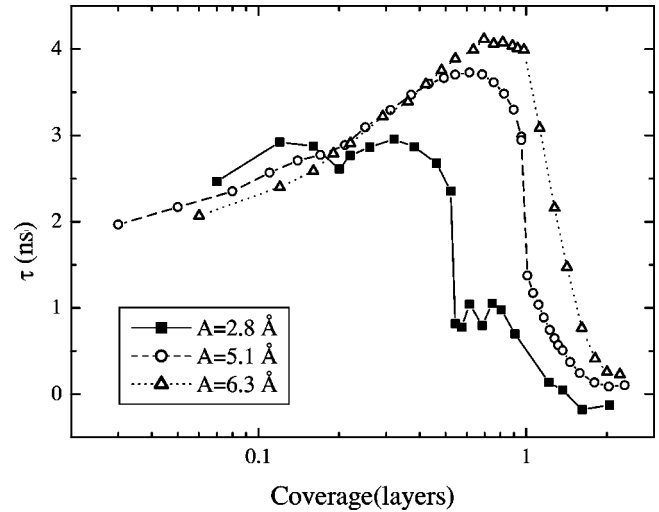


FIG. 5. Coverage scans of Kr on gold measured with quartz 2 at 97 K for three different amplitudes of oscillation.

age. Figure 6 shows datasets relative to three different sub-monolayer coverages, obtained with quartz 2 at the temperature of 97 K. The top graph contains data acquired while increasing the amplitude of oscillations, while the bottom one displays the corresponding scans taken by decreasing  $A$  back to zero. (We have decided to split the scans in two plots only for clarity reasons.) The data at increasing  $A$  show distinctly that the depinning of the film from the substrate occurs at different values of  $A$ , depending on the coverage. They also confirm that sliding is favored at lower coverages: the depinning threshold increases with film coverage. The pinning transition is instead significantly lower than the corresponding value measured while increasing  $A$ . We have already observed the same hysteresis analyzing data acquired using crystal 1.<sup>14</sup>

This experimental observation of the transition from static to dynamic friction is in good qualitative agreement with extensive computer simulations based on the Langevin equa-

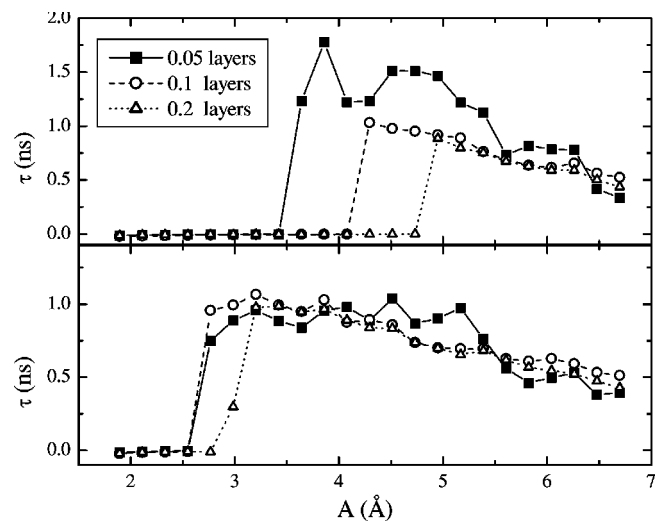


FIG. 6. Amplitude scans of Kr on gold acquired using quartz 2 at 97 K for three coverages.

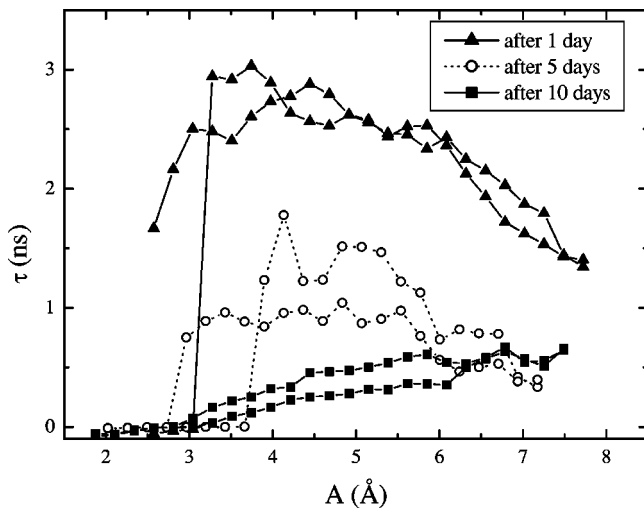


FIG. 7. Amplitude scans corresponding to a film of 0.05 layers measured with quartz 2 at 97 K and obtained by repeating the measurement after 1, 5, and 10 days from the first cool down.

tion carried out by Persson, who found similar hysteresis loops in his study of a model system of molecules adsorbed on a regular lattice and subject to a tangential force.<sup>9</sup> In this model, the adsorbate molecules interact with each other via a Lennard-Jones pair potential and the adsorbate-substrate interaction potential is assumed to be a simple cosine corrugation along the two planar directions  $x$  and  $y$ . The observed hysteresis and nonlinearity with respect to the external applied force are explained in terms of the melting of a solid commensurate film. As the driving amplitude increases from zero, the ordered structure prevails and there is no sliding until  $A$  reaches a certain critical value. At this depinning value, the sliding velocity increases abruptly and the film becomes fluidlike. When decreasing  $A$ , the film goes back to its initial state at a much lower amplitude. The return to the pinned state is found to be a nucleation process.

Needless to say, a more quantitative comparison between experiment and simulation is not possible at this stage. The reasons are simply that the theoretical model is probably too simple and that our gold surface is not regular. The electrodes evaporated in vacuum are likely to have a polycrystalline surface with a (111) texture, chemically pure but with a rough profile and possibly covered during the experiments by some foreign particles which may act as pinning centers. Actually, depinning transitions observed with different quartz crystals at the same nominal conditions suggest that the microscopic state of the electrodes surface plays a major role in our measurements as expected. Data taken with the same quartz crystal but at different times may also look somewhat different. For example, the adsorption isotherms reported in Fig. 5 always show sliding of Kr for coverages  $\leq 0.4$  layers and amplitudes greater than  $2.8 \text{ \AA}$  with a characteristic slip time  $\sim 2 \text{ ns}$ . Instead, the amplitude scans indicate that for  $A = 2.8 \text{ \AA}$  there is pinning of a 0.2-layer film and sliding of thinner films but with  $\tau \sim 1 \text{ ns}$ . These two sets of data have been taken in different weeks and this may have caused a change in the gold surface.

Figure 7 further corroborates such an interpretation. It

represents amplitude scans taken with quartz 2 at the same nominal experimental conditions but in different days. During this period of time, the experiment has been always kept at low temperature and several measurements have been carried out at different temperatures and film coverages. Right after a cool down, on a fresh gold surface, a sharp depinning transition is observed to occur at  $A = 3 \text{ \AA}$ . After five days, the transition has moved to  $A = 3.7 \text{ \AA}$  and the slip time has decreased by a factor of 2. Finally, after 10 days, the transition is very broad and  $\tau \leq 0.5 \text{ ns}$ . The progressive disappearance of the depinning transition is probably caused by the deposition onto the gold electrodes of foreign molecules which likely act as pinning centers. Actually, after these runs the resonance frequency in vacuum decreased by  $\sim 2 \text{ Hz}$  with respect to the initial value right after the cool down. We believe that these impurities are mainly due to the outgassing of the gas system and dosing tubes which are pumped down to  $10^{-6} \text{ Torr}$ . Contamination from the dosing gas is unlikely given its high purity (scientific grade) and the use of a cold trap in the gas handling system. For a more systematic study of this effect, it would be necessary to quantify the surface defects with, for example, an AFM/STM probe; unfortunately, with our current setup we cannot do it.

## V. CONCLUSIONS

We have employed the quartz-crystal microbalance technique to measure nonlinear sliding friction of thin Kr films adsorbed on gold substrates. A novel normalization procedure of the slip time has been introduced to account for the dynamic response of thin films in the submonolayer region. By increasing the oscillating amplitude of the quartz electrodes and, accordingly, the force of inertia acting tangentially on the Kr atoms, a transition from static to dynamic friction has been observed with two different quartz crystals. As the driving amplitude is decreased back to zero, the slip time describes a pronounced hysteresis loop, similar to what found in computer simulations. Quantitative comparisons between the nanofriction data acquired with the two quartz plates at the same nominal conditions suggest that the morphology of the surface electrodes strongly affect these phenomena. The influence of the surface defects has been more directly observed through the progressive disappearance of the depinning transition with time, which shows that the contamination of the gold surface by foreign particles drastically reduces the slippage. We would like to conclude by pointing out that a more comprehensive understanding of these phenomena requires the use of very homogeneous and well characterized surfaces and the measurements must be performed in a UHV environment.

## ACKNOWLEDGMENT

This work has been supported by Università di Padova and INFN-PRA Nanorub.

- <sup>1</sup>See, e.g., D. Fisher, *Phys. Rep.* **301**, 113 (1998).
- <sup>2</sup>M.C. Marchetti, A.A. Middleton, and T. Prellberg, *Phys. Rev. Lett.* **85**, 1104 (2000); J.M. Schwarz and D.S. Fisher, *ibid.* **87**, 096107 (2001).
- <sup>3</sup>G. Blatter, M.V. Feigel'man, V.B. Geshkenbein, A.I. Larkin, and V.M. Vinokur, *Rev. Mod. Phys.* **66**, 1125 (1994).
- <sup>4</sup>G. Grüner, *Rev. Mod. Phys.* **60**, 1129 (1988).
- <sup>5</sup>E. Rolley, C. Guthmann, R. Gombrowicz, and V. Repain, *Phys. Rev. Lett.* **80**, 2865 (1998).
- <sup>6</sup>A. Glatz, T. Nattermann, and V. Pokrovsky, *Phys. Rev. Lett.* **90**, 047201 (2003).
- <sup>7</sup>C. Reichhardt and C.J. Olson, *Phys. Rev. Lett.* **89**, 078301 (2002).
- <sup>8</sup>See, e.g., B. N. J. Persson, *Sliding Friction* (Springer-Verlag, Berlin, 1998); *Physics of Sliding Friction*, edited by B. N. J. Persson and E. Tosatti (Kluwer, Dordrecht, 1996); *Tribol. Lett.* **10** (2001).
- <sup>9</sup>B.N.J. Persson, *Phys. Rev. Lett.* **71**, 1212 (1993); *Phys. Rev. B* **48**, 18 140 (1993); *J. Chem. Phys.* **103**, 3849 (1995).
- <sup>10</sup>P.A. Thompson and M.O. Robbins, *Science* **250**, 792 (1990).
- <sup>11</sup>O.M. Braun, T. Dauxois, M.V. Paliy, and M. Peyrard, *Phys. Rev. Lett.* **78**, 1295 (1997).
- <sup>12</sup>E. Granato and S.C. Ying, *Phys. Rev. Lett.* **85**, 5368 (2000).
- <sup>13</sup>C.M. Mate and B. Marchon, *Phys. Rev. Lett.* **85**, 3902 (2000).
- <sup>14</sup>L. Bruschi, A. Carlin, and G. Mistura, *Phys. Rev. Lett.* **88**, 046105 (2002).
- <sup>15</sup>J. Krim, *Sci. Am. (Int. Ed.)* **275**, 74 (1996).
- <sup>16</sup>L. Bruschi and G. Mistura, *Phys. Rev. B* **63**, 235411 (2001).
- <sup>17</sup>L. Bruschi, G. Delfitto, and G. Mistura, *Rev. Sci. Instrum.* **70**, 153 (1999).
- <sup>18</sup>K.K. Kanazawa, *Faraday Discuss.* **107**, 77 (1997); B. Borowsky, B.L. Mason, and J. Krim, *J. Appl. Phys.* **88**, 4017 (2000).
- <sup>19</sup>J. Krim and A. Widom, *Phys. Rev. B* **38**, 12 184 (1988); E.T. Watts, J. Krim, and A. Widom, *ibid.* **41**, 3466 (1990).
- <sup>20</sup>J. Krim, D.H. Solina, and R. Chiarello, *Phys. Rev. Lett.* **66**, 181 (1991).
- <sup>21</sup>B. N. J. Persson, *Sliding Friction* (Ref. 8), pp. 31–35.